Tuning the electronic and structural properties of supported iron oxide catalysts

Key-words: Hydrodeoxygenation, Iron Oxide, Oxide-support interaction

Authors:

Pedro Becchelli de Moraes Nunes, IQ/Unicamp

Gabriel de Biasi Báfero, IQ/Unicamp

Profª. Drª. Daniela Zanchet (advisor), IQ/Unicamp

INTRODUCTION

Supporting metal or metal oxide phases in a matrix, generally a high surface area oxide, is a key methodology to enhance the performance of a catalyst in different reactions. The high surface area of the support is expected to provide a better dispersion of the active phase, giving rise to more stable and active catalysts with tunable structural and electronic properties [1-3].

The supports, however, can present their own activity, with acidic, redox, and electronic properties strongly affecting the characteristics of the resulting material[1,2]. Unique interfacial interactions can arise, usually called MSI (metal-support interaction), such as charge transfer[4,5] or surface structural variations[6].

In the context of biomass upgrading, one of the most important catalytic processes is the hydrodeoxygenation (HDO) reaction, which aims to reduce the oxygen content of lignocellulosic bio-oils, a mixture of different oxygenated molecules (ketones, aldehydes, sugars, etc)[6,7]. This can be achieved through the selective cleavage of C-O bonds of the substrate under a H_2-rich atmosphere, along a heterogeneous catalyst. However, due to the high complexity of the bio-oils' composition, model compounds, such as acetone[8-10], are often employed to simplify the methodology and the identification of preferred pathways[11]. We showed previously that iron oxide nanopowder yielded interesting results in the acetone HDO[12] by tuning the oxidation states of iron ($Fe^0/Fe^{2+}/Fe^{3+}$) through thermal pre-treatments, which increased both the activity and selectivity towards C-O cleavage. However, a low acetone:catalyst ratio was employed to achieve significant conversions, which can be attributed to the low activity of bulk iron oxide. A WHSV (see eq. 1) of 0.94 h^{-1} resulted in acetone conversions from 20 to 60 %.

Thus, in this work, we prepared supported iron oxide catalysts for the acetone HDO reaction. We aimed to investigate the influence of supports with different acidic and redox characters, namely γ-Al_2O_3 (acid), SiO_2 (inert), $MgAl_2O_4$ (basic), TiO_2 and CeO_2 (redox) by conducting screening catalytic tests with the synthesized catalysts.

EXPERIMENTAL

Materials

Acetone (≥ 99.9%, HPLC Plus Grade), γ-Fe_2O_3 (<50 nm particle size), $Fe(NO_3)_3.9H_2O$, γ-Al_2O_3 and CeO_2 were purchased from Sigma-Aldrich. SiO_2 - Aerosil 380 was purchased from Evonik. MgAl Oxide Hydroxide, purchased from Sasol, was calcined at 800 ºC/5h to produce $MgAl_2O_4$. TiO_2-P25 was acquired from Degussa. Reactions and pretreatments were conducted in a quartz reactor, accommodating a quartz wool bed.

Synthesis

Incipient wetness impregnation (IWI): The catalysts were prepared by adding an appropriate amount of $Fe(NO_3)_3$ solution dropwise to the supports (SiO_2, γ-Al_2O_3, and $MgAl_2O_4$) under vigorous mechanical mixing, to reach a loading of 21.3 Fe at. % (about 20 wt. %). The samples were then dried at 90 ºC overnight and calcined at 500 ºC for 4 h. The resulting catalysts were named Fe/SiO_2, Fe/Al_2O_3 and $Fe/MgAl_2O_4$.

Wet impregnation (WI): The catalysts were prepared by dissolving an appropriate amount of $Fe(NO_3)_3$ in 10 ml of water, which was then dispersed in an ultrasonic bath for 30 min. The supports (SiO_2, TiO_2 and CeO_2) were passed through a 100 mesh sieve, then added to the beaker containing the precursor, which was heated to 60 ºC until all solvent was evaporated. The samples were then dried at 90 ºC overnight and calcined at 500 ºC for 4 h. The resulting catalysts were named Fe/SiO_2, Fe/TiO_2 and Fe/CeO_2. The samples were also reduced with 30 % hydrogen at 550 ºC, 30 min isothermal, being named Fe/support_red.

Catalytic Evaluation

HDO screenings were performed from 100 to 450 ºC, with 50 ºC steps, isothermal during 30 min. The thermal pre-treatments and catalytic tests were conducted in a continuous quartz reactor, with a quartz wool bed. For the supported catalysts, 50 mg of catalyst were used for the reactions, homogeneously mixed with 150 mg of quartz powder as diluent, resulting in a WHSV (weight hourly space velocity) of 11.23 h^{-1}. This value can be obtained by the following equation:

$$WHSV = \frac{Acetone\ mass/time\ (g.h^{-1})}{Catalyst\ mass\ (g)} = \frac{0.56\ g.h^{-1}\ of\ Acetone}{0.05\ g\ of\ catalyst} \textbf{ (eq.1)}$$

For the HDO using γ-Fe_2O_3 nanopowder, 14.3 mg was used which contains approximately 10 mg of Fe.

The mass of acetone was deduced considering the temperature of the saturator, 10 ºC (283 K), and a 3.62 mL min^{-1} flow, while using the ideal gas law. It was fed into the reactor through a saturator and carried by 20 mL min^{-1} of He. 76.38 mL min^{-1} of H_2 were employed to reach a 21:1 molar ratio of hydrogen to acetone reaching a total flow of 100 mL min^{-1}.

Acetone conversion and products' selectivity (eq. 2 and 3, respectively) were monitored by an on-line gas chromatograph (GC - Agilent Technologies, model 7890A) equipped with an HP-1 column (50 m x 0.32 mm i.d., 0.17 μm). The main detected products were methane (C1), ethylene (C2), propylene (C3E), propane (C3A), isobutene (C4), isopropanol (IPA), methyl-pentane, hexene and isomers (C6), cyclohexane and isomers (cC6), benzene, toluene and xylene (BTX), nonene and isomers (C9), mesityl oxide (C6O) and 2,6-dimethyl-4-heptanone (C9O). Except when stated otherwise, all carbon balances obtained were higher than 0.9.

$$Acetone\ conversion\ (\%) = 100 \times \frac{moles\ of\ acetone\ consumed}{moles\ of\ acetone\ fed} \quad \textbf{(eq. 2)}$$

$$Distribution\ to\ a\ product\ (\%) = 100 \times \frac{produced\ moles\ of\ the\ product}{moles\ of\ acetone\ consumed} \quad \textbf{(eq. 3)}$$

$$DD\ (\%)\ =\ sum\ of\ the\ distributions\ to\ C_n,\ n \geq 3 \textbf{(eq.4)}$$

RESULTS AND DISCUSSION

XRD measurements

Figure 1 shows the XRD patterns for the (a) IWI and (b) WI 21.3 Fe at.% prepared catalysts, as well. They were conducted to obtain information about the dispersion of the Fe phases over the supports, and were compared to α-Fe$_2$O$_3$ (ICSD collCode 71194)
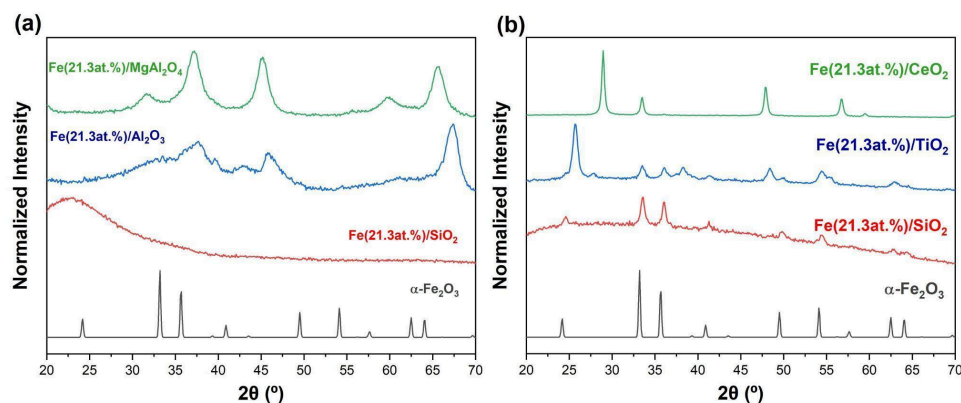

Figure 1: XRD patterns of the 21.3 Fe at. % supported catalysts prepared by (a) IWI and (b) WI. The α-Fe$_2$O$_3$ diffraction pattern is shown as reference.

The obtained XRD patterns for the IWI samples pointed to the presence of well dispersed surface FeO$_x$ species, since the diffraction peaks (or amorphous halo, for SiO$_2$) essentially correspond to the supports' crystalline structure. Scanning Electron Microscopy (SEM, not shown), revealed no recognizable or characteristic iron domains, while the Energy Dispersive Spectrometry (EDS) analysis revealed poor dispersion of the iron phases, with some regions having atomic % as low as 3.3% and as high as 28.6%, leading to an average at.% with a standard deviation that represents 79% of the measurement.

Regarding the WI samples, the CeO$_2$-supported catalyst had no apparent peaks regarding FeO$_x$ phases, while the TiO$_2$- and SiO$_2$-supported ones presented peaks related to α-Fe$_2$O$_3$, the expected phase resulting from a calcination at 500 ºC. Although the XRD results show the formation of crystalline iron phases over SiO$_2$ and TiO$_2$, the following catalytic data and SEM of IWI-prepared Fe/SiO$_2$ indicates that WI was more efficient in impregnating the support's surface than IWI. Using Scherrer's equation, the crystallites had an average size of 16.6 nm and 13.1 nm for the silica- and titania-supported catalysts, respectively.

Catalytic Evaluation

IWI catalysts: The performance of the fresh supported 21.3 at.% catalysts in the acetone HDO reaction as a function temperature is exhibited by **Figure 2**. For comparison, the test was also performed with an equivalent mass of nanopowder γ-Fe$_2$O$_3$ (bulk catalyst).
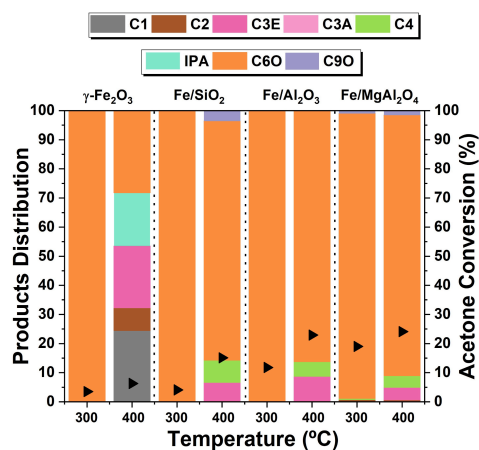
Figure 2 : Products distribution (bars, left axis) and acetone conversion (triangles, right axis) for the HDO reaction as a function of temperature, using the fresh 21.3 Fe at.% IWI catalysts.

No catalyst was selective towards deoxygenated products at 300 °C, being completely selective towards C6O. At 400 °C, all of the catalysts yielded deoxygenated products, with DD as follows: Fe/SiO$_2$ (14.4 %) > Fe/Al$_2$O$_3$ (13.9 %) > Fe/MgAl$_2$O$_4$ (8.4 %). The SiO$_2$ supported catalyst was, however, the least active, reaching 15.1 % in acetone conversion, whereas Al$_2$O$_3$ had 22.9 % and MgAl$_2$O$_4$ 24.1 %. The reduced IWI catalysts were also evaluated at these conditions, where results were highly similar to the untreated materials.

WI catalysts: **Figure 3** presents the performance of the (a) fresh and (b) reduced supported 21.3 at.% catalysts in the acetone HDO reaction as a function temperature, as well as the nanopowder γ-Fe$_2$O$_3$ for comparison.
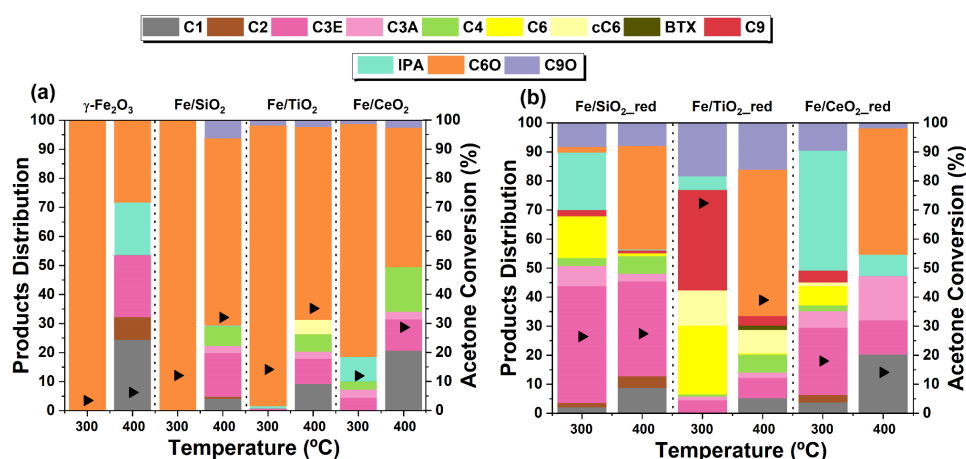
Figure 3 : Products distribution (bars, left axis) and acetone conversion (triangles, right axis) for the HDO reaction as a function of temperature, using the (a) fresh and (b) reduced 21.3 Fe at.% WI catalysts.

At 300 °C, only Fe/CeO$_2$ presented any activity towards non-condensation products, which, however, can be attributed to the support. At 350 °C and higher all the catalysts were capable of producing deoxygenated products, with conversions higher than 20 %, already surpassing the maximum obtained for γ-Fe$_2$O$_3$. Fe/SiO$_2$ obtained by WI was superior to the one prepared by IWI, generating up to 45% of deoxygenated products and reaching conversions of 31.9 %, twice the achieved previously.

Fe/TiO$_2$ had the highest DD at 400 ºC, reaching more than 22%, while Fe/TiO2_red had a unique products' distribution at 300 ºC, majorly C3, C6, cC6 and of C9, as well as the highest DD 76.8 % and the conversion (58.7 %) of all the catalysts. The production of C9, cC6 and other cyclic products was only observed in titatina-supported catalysts, pointing to the occurrence of MSI between Fe and TiO$_2$.

CONCLUSIONS

The catalytic performance of fresh and reduced Fe(21.3 at.%)/support was screened from 300 ºC to 400 ºC on the gas-phase hydrodeoxygenation reaction of acetone, with catalysts prepared by IWI on SiO$_2$, Al$_2$O$_3$ and MgAl$_2$O$_4$ and by WI on SiO$_2$, TiO$_2$ and CeO$_2$.

Although the fresh IWI supported catalysts surpassed the γ-Fe$_2$O$_3$ nanopowder in terms of activity and DD, the catalysts performed very similarly to one another, with no significant deviations while working with materials with considerably different properties. The catalytic tests, correlated with the SEM-EDS data collected, led us to question the effectiveness of the impregnation process and prompted us to attempt impregnation by the wet method (WI). A catalytic comparison between the silica-supported catalysts prepared by the two methods indicates that the WI was more effective in impregnating the support's surface, which could be confirmed through more extensive characterization of the WI samples.

Overall, the reduced catalysts were the most active and selective where the use of different supports favored different pathways that led to specific products: direct deoxygenation products (C3) for Fe/SiO$_2$_red and Fe/CeO$_2$_red, and C-C coupling (C6, C9) and cyclic (cC6) products for Fe/TiO$_2$_red. This points to the occurrence of different MSI, which we plan to elucidate by the characterization of surface species by XPS and post-reaction XRD.

BIBLIOGRAPHY

[1] Carl R. F. Lund and J. A. Dumesic. Journal of Physical Chemistry, 1981, 85 (21), 3175-3180. doi.org/10.1021/j150621a034

[2] van Deelen, T.W. et al. Nature Catalysis. 2, 955–970 (2019). doi.org/10.1038/s41929-019-0364-x

[3] Shetty, M et al. Journal of Catalysis, 2015, vol. 331, 86-97. doi.org/10.1016/j.jcat.2015.07.034

[4] Puigdollers, A. R., et al. ACS Catalysis 7, 6493–6513 (2017). doi.org/10.1021/acscatal.7b01913

[5] Pacchioni, G.. Physical Chemistry Chemical Physics, 15, 1737–1757 (2013).doi.org/10.1039/C2CP43731G

[6] M. Boudart, Advances in Catalysis 20, 1969, 153-166. doi.org/10.1016/S0360-0564(08)60271-0

[7] Montoya, J. I. et al. Dyna UNAL, 2015, 82, 192, 239-248. doi.org/10.15446/dyna.v82n192.44701

[8] Leite, D. S. et al. Molecular Catalysis, 2022, 530, 112623. doi.org/10.1016/j.mcat.2022.112623

[9] Báfero, G. B. et al. ChemCatChem, 2023, 15, 16. doi.org/10.1002/cctc.202300663

[10] Strapasson, G. B. et al. Applied Catalysis B, 2023, 122863. doi.org/10.1016/j.apcatb.2023.122863

[11] Mortensen, P. M. et al. Applied Catalysis A, 2011, 407, 1-2, 1-19. doi.org/10.1016/j.apcata.2011.08.046

[12] Nunes, P. B. M et al. JBCS: Solid State Chemistry, 2024, 1-11. doi.org/10.21577/0103-5053.20240126